Realistic Spatio-Temporal Channel Model for Broadband MIMO WLAN Systems Employing Uniform Circular Antenna Arrays

M. A. Mangoud and Z. Mahdi

Department of Electrical and Electronics Engineering,
University of Bahrain, P. O. Box 32038, Isa Town, Kingdom of Bahrain
Mangoud@ieee.org

Abstract ─ The development of realistic spatially and temporally clustered channel models is a prerequisite to the creation of successful architectures of the future MIMO wireless communication systems. IEEE 802.11n channel models are designed for indoor wireless local area networks for bandwidths of up to 100 MHz, at frequencies of 2 and 5 GHz. The channel models comprise a set of 6 realistic profiles, labeled A to F, which cover the scenarios of flat fading, residential, residential/small office, typical office, large office, and large space. Each channel scenario is represented by distinct path loss model, multipath delay profile, number of clusters and taps with predefined values for angular and power parameters. These realistic models have been applied widely for MIMO systems utilizing only uniform linear array (ULA). In this paper, modifications to the standard IEEE 802.11n channel model are applied to include uniform circular array (UCA) geometries. Characteristics of spatial fading corrections and the eigenvales distribution of subchannels for UCA-MIMO systems are investigated. The effect of the azimuth orientation and line of sight component existence on the system capacity for both ULA and UCA arrays are studied. Also, the water filling power allocation scheme is investigated under different realistic conditions. Furthermore, the link performance of Vertical Bell Laboratories Layered Space Time (VBLAST) that employs UCA at the receiver front is presented by utilizing the developed channel model.

I. INTRODUCTION

Multiple input multiple output (MIMO) technology offers a spatial diversity that can be utilized to achieve significant capacity gain as well as improve system performance [1]. Most of the studies for the design and performance evaluation of MIMO wireless communication systems use simplified statistical channel models that are idealized abstractions of temporal and spatial correlations [2-3]. The main limitation of these channel models is that realistic channel conditions are not included as they provide simple and intuitive relations to physical directions and propagation environments. Various measurements show that realistic MIMO channels provide different capacity values [4-5]. Therefore, developing accurate and realistic correlated channels is essential and of crucial importance to predict an accurate performance of MIMO systems. Some realistic models are proposed as standardized channel models were unified and agreed on by many scientific parties worldwide to be used in the development of modern MIMO systems. The most commonly used standard spatial channel models for system level simulations are the 3GPP/3GPP2 SCM (spatial channel model) [6] for outdoor cellular wide area scenarios and the Technical Group of IEEE 802.11 TGn channel model [7] for indoor WLAN short range scenarios. The two models assume that transmitter and receiver MIMO antennas are restricted to uniform linear arrays (ULAs). However, recently there has been increased interest in using uniform circular arrays (UCAs) [8-14], which is perhaps the next most common array geometries for future generation WLANs

due to their enhanced azimuth coverage. Therefore, in this paper, we extend our work in [14] and develop a more realistic spatially and temporally clustered channel model to be applied in the simulation of UCA-MIMO systems for WLANs. The proposed model accounts for six different actual propagation scenarios that are applied in IEEE802.11 TGn channel model. Numerical simulation examples are performed for different case studies to investigate system capacity and BER performance of the pre-set realistic scenarios. The rest of the paper is organized as follows. Section 2 describes the developed channel model and the modifications proposed to the existing IEEE802.11n standard model to include UCA configurations. Section 3 provides the temporal properties of the clustered MIMO channel models. In section 4 numerical results are discussed and a thorough discussion about the applicability of the developed model is presented. Finally, conclusions are given in section 5.
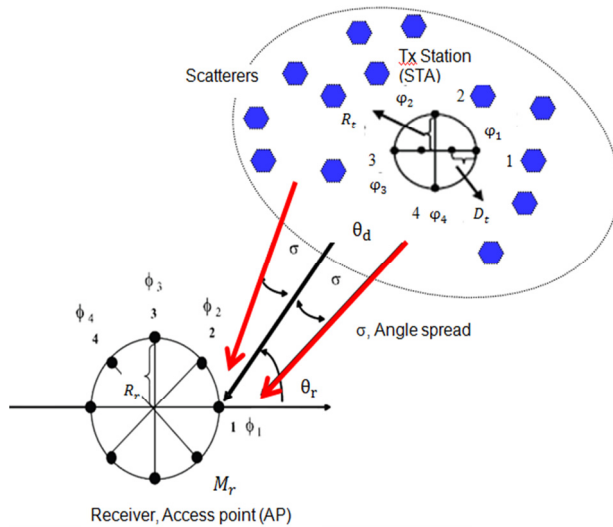

Fig. 1. MIMO communication system employing ($M_t \times M_r$) ULA / UCA configurations.

II. MODIFIED SPATIAL CHANNEL MODELS

Considering an uplink of IEEE802.11*n* MIMO WLAN communication system operating in an indoor environment, where the transmitter is a wireless station (STA) and the receiver is an access point (AP). Figure 1 shows ($M_t \times M_r$) MIMO WLAN system with M_t -element transmit-antenna array at STA and M_r -element receive-antenna array at AP end. We consider the arrays at STA and AP to be either ULA with inter-element spacing D_t and D_r or UCA of radius R_t and R_r, respectively. The figure also shows a graphical representation of the clustered channel model where the angle that each *i*-th element location makes with the horizontal axis is denoted as φ_i and ϕ_i for transmitter and the receiver. The central angle of departure (AoD) and the central angle of arrival (AoA) are θ_d and θ_r, respectively. Additionally, it is assumed that the channel is composed of several moving scatterers which are local to STA. Thus, the received signal is the sum of multiple plane waves with random phases. Under this assumption, the channel consists of multiple sample taps, which are associated with different clusters. The discrete-time impulse response of MIMO channel matrix can be written as in [7]:

$$\mathbf{H}(t) = \sum_{l=1}^{L-1} \mathbf{H}_l(t)\delta(t - \tau_l), \qquad (1)$$

where t denotes the discrete time index, L is the number of effectively nonzero channel taps (corresponding to the channel clusters), $\mathbf{H}_l(t)$ is the $M_t \times M_r$ channel matrix for the *l*-th tap, $\delta(t - \tau_l)$ is the Kronecker delta function for τ_l delay at *l*-th tap. For simplicity, notation t will be omitted in the following equations. The *l*-th matrix tap $\mathbf{H}_l$ at one instance of time can be written as the sum of a constant line of sight (LOS) matrix and a variable Rayleigh non line of sight (NLOS) matrix

$$\mathbf{H}_l = \sqrt{p_l}\left\{\sqrt{\frac{K_l}{K_l+1}}\left[e^{j2\pi\left(\frac{v_o}{\lambda}\right)t\cos\left(\frac{\pi}{4}\right)}.\mathbf{S}\right] + \sqrt{\frac{1}{K_l+1}}\left(\mathbf{R}_{\mathbf{spatial}}.\mathbf{B}\right)\right\}, \qquad (2)$$

where the first term represents $\mathbf{H}_l^{LOS}$ and the second accounts for $\mathbf{H}_l^{NLOS}$, p_l is the total power of l-th channel tap that is the sum of the fixed LOS power and the variable NLOS power of the *l*-th tap defined in the power delay profiles, K_l is the Rician *K*-factor of *l*-th tap that represents the relative strength of the LOS component, $\mathbf{S}$ is the steering matrix, $\mathbf{R}_{spatial}$ is spatial fading correlation shaping matrix, $\mathbf{B}$ is a vector that is

obtained by passing $\mathbf{H}_{iid}$ independent complex Gaussian random samples with zero mean and unit variance through a filter that is shaped based on the Doppler model where the transmitter and receiver are stationary and the surrounding objects and people are moving, the exponential term is used to account for the phase change introduced in the LOS path due to the movement of scattering objects with velocity v_o that is assumed to be fixed at 1.2 kmph. The model is adopted to include UCA configurations at both STA and AP ends by defining the steering vector used in (2) as

$$\mathbf{S} = \begin{pmatrix} e^{j2\pi\left(\frac{R_t}{\lambda}\right)\sin(\zeta)\cos(\theta d - \varphi_1)} \\ \vdots \\ e^{j2\pi\left(\frac{R_t}{\lambda}\right)\sin(\zeta)\cos(\theta d - \varphi_{Mt})} \end{pmatrix}^T .$$

$$\begin{pmatrix} e^{j2\pi\left(\frac{R_r}{\lambda}\right)\sin(\zeta)\cos(\theta r - \phi_1)} \\ \vdots \\ e^{j2\pi\left(\frac{R_r}{\lambda}\right)\sin(\zeta)\cos(\theta r - \phi_{Mr})} \end{pmatrix}, \quad (3)$$

where λ is the signal wavelength, ζ is the elevation angle. For simplicity, only azimuth angles are considered in the propagation geometry (i.e., $\zeta = 90^o$), however the results can be generalized to three dimensions by changing the value of ζ. Note that, the extra distance that the signal has to travel from adjacent antenna elements at the transmitter end is $R_t \cos(\theta - \varphi_i)$ that results in a phase difference of $(2\pi\frac{R_t}{\lambda})\cos(\theta - \varphi_i)$. A similar phase shift term is included at the receiver. It should be noted that the AoA and AoD for the LOS path of the channel are assumed to be fixed at 45 degrees. According to [8] and [14], the correlation between m-th and n-th element in

$$R(m,n) = \int_{-\pi}^{\pi} e^{j(\varphi_m - \varphi_n)} P_\theta(\theta) \, d\theta, \quad (4)$$

where $P_\theta(\theta)$ is the power azimuth spectrum (PAS) distribution that has a truncated Laplacian shape, θ is either θ_d or θ_r the central random variable for AoD or AoA, where $R(m,n)$ is the complex correlation coefficients between the m-th and n-th antennas. Thus, the complex spatial correlation matrix $\boldsymbol{R}_{rx}$ at the receiver end with UCA configuration is obtained by numerically performing the integral in (4) as in [8]

$$Re\{R_{rx}(m,n)\} = J_o(Z_c)$$

$$+2\sum_{k=1}^{\infty} \frac{a^2(1-e^{-a\pi})}{a^2+4k^2} J_{2k}(Z_c)\cos[2k(\theta_r + \alpha)], \quad (5)$$

$$Im\{R_{rx}(m,n)\} = \frac{2a}{(1-e^{-a\pi})}\sum_{k=0}^{\infty} \frac{a(1-e^{-a\pi})}{a^2+(2k+1)^2} \cdot$$
$$J_{2k+1}(Z_c)\sin[(2k+1)(\theta_r + \alpha)], \quad (6)$$

where a is a decay factor which is related to the angle spread, when a increases the angle spread decreases, α is the relative angle between the m-th and n-th antenna elements, Z_c is related to the antenna spacing and is defined as follows

$$Z_c = \sqrt{\begin{array}{c}(2\pi\left(\frac{R_r}{\lambda}\right)\{[\cos\varphi_m - \cos\varphi_n]^2 \\ + [\sin\varphi_m - \sin\varphi_n]^2\}\end{array}} . \quad (7)$$

A similar expression can be obtained for $\boldsymbol{R}_{tx}$ coefficients as in (5) and (6) by replacing θ_r, R_r, φ_m, φ_n with θ_d, R_t, ϕ_m, ϕ_n respectively.

III. TEMPORAL PROPERTIES OF CHANNEL MODEL

In the temporal domain, the properties of the proposed MIMO channel models for systems employing UCA configurations are assumed to be similar to the clustered model that was first introduced by Saleh and Valenzuela in [2]. The model is based on assuming that the received signal comprises of multiple decayed rays (clusters) that were reflected from different groups of scatterers. The received signal is assumed to be a summation of different exponential functions in time. For the given assumptions, the impulse response of the channel can be expressed as:

$$h(t) = \sum_{l=0}^{\infty}\sum_{k=0}^{\infty} a_{kl}\delta(t - T_l - \tau_{kl}), \quad (8)$$

where T_l is the arrival time of the first ray of l-th cluster. τ_{kl} is the arrival time of the k–th ray within the l-th cluster. a_{kl} is the amplitude of each arriving ray, which is a Rayleigh distributed random variable with mean square value equal to

$$\overline{a_{kl}^2} = \overline{a^2(T_l, \tau_{kl})} = \overline{a^2(0,0)}\, e^{-T_l/\Gamma}\, e^{-\tau_{kl}/\gamma}, \quad (9)$$

where $a^2(0,0)$ is the average power of the first ray of the first cluster and depends on the distance between the transmitter and receiver, Γ is the cluster power decay time constant and γ is the ray

power decay time constant within a cluster. For the developed model, the clusters and taps exponential decays are not used, instead values for the power delay profiles that will be used throughout the paper are defined as in [7] for standard IEEE 802.11*n* channel models as shown in Table 1.

Table 1: IEEE802.11n TGn channel models [7]

Mo del	Environment	K (dB) LOS/NLOS	Delay (rms)	Clusters
A	Flat fading	0/-∞	0	1
B	Residential	0/-∞	15	2
C	Residential/ small office	0/-∞	30	2
D	Typical Office	3/-∞	50	3
E	Large Office	6/-∞	100	4
F	Large Space, In-/out-door	6/-∞	150	6

The system capacity is defined as the maximum possible transmission rate such that the probability of error is arbitrarily small. By applying the singular value decomposition (SVD) theorem, the ergodic capacity (C) in the case of the uniform power scheme is given by

$$C = E\left\{ W \sum_{i=1}^{r} \log_2 \left[1 + \frac{P_i \lambda_i}{\sigma^2} \right] \right\}, \qquad (10)$$

where $E\{.\}$ Is the expectation operator, r is the rank of the $M_t \times M_r$ channel matrix **H**, where W is the bandwidth of each sub-channel, P_i is the received signal power in the i-th sub-channel that is equal to P/M_t, P is the total power, λ_i is the eigenvalue of the sub-channels, σ^2_n is the noise power. In this case, the power is equally divided among the transmit antennas. However, when applying the water-filling (WF) power scheme that is the optimal energy allocation algorithm [1]. The power values P_i are assigned on the basis that the better the sub-channel gets, the more power is injected into it and the ergodic capacity in this case will be

$$C = E\left\{ W \sum_{i=1}^{r} \log_2 \left[1 + \frac{\lambda_i}{\sigma^2} (\mu - \frac{\sigma^2}{\lambda_i})^+ \right] \right\}, \qquad (11)$$

where a^+ denotes max$(a, 0)$, $i= 1, 2, \ldots, r$ and μ is determined so that $\sum_{i=1}^{r} P_i = P$.

IV. NUMERICAL RESULTS AND ANALYSIS

In this section, we study and compare the channel capacity and system performance of UCA-MIMO WLAN systems using the numerically developed realistic channel model. Unless specified, the MIMO system (4×4) are considered, both ends utilize the UCA configuration with radius 0.5 or 0.75 wavelength spacing. 10000 channel realizations and NLOS scenario with SNR=10 dB are considered. If ULA configuration is being used then the inter-elements spacing is considered to be 0.5λ. The six standard *TGn* channel model profiles (A-F) defined in [7] are used here to realize realistic scenarios throughout the following simulation study cases. Figure 2 shows probability density function (*pdf*) of the AoA for model 'F' and shows how the power is distributed among the taps and the clusters. The model has 5 overlapping clusters with 18 taps. All taps *pdf* are considered as truncated laplacian functions [7].
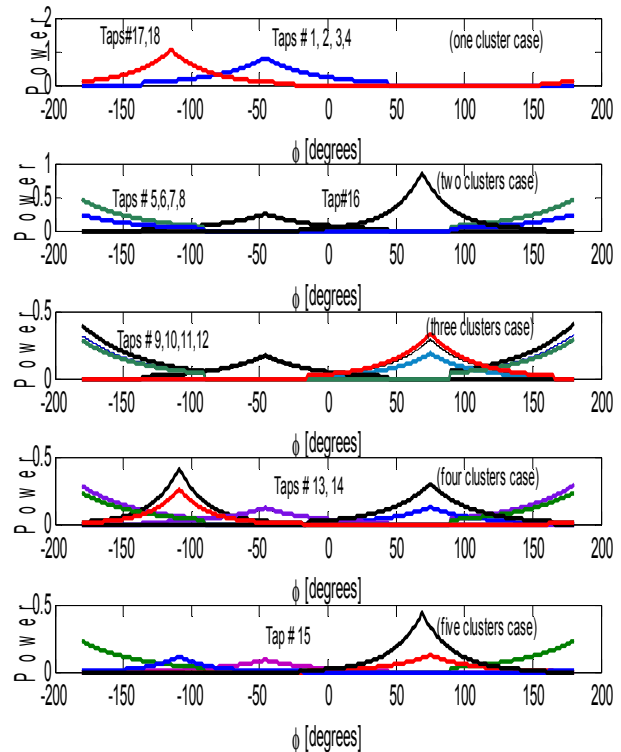

Fig. 2. *pdf* of the AoA for the taps in model 'F'.

Figure 3 illustrates the channel spatial correlation R_s (21, 11) between the links h_{11} and h_{21} for all taps of model 'F' versus the UCA radius

in the receiver. It is obvious that the spatial correlation decreases as UCA antenna radius increases. In addition, one can see that the spatial correlation differs for various taps depending on AoA and the angular spread (AS) of each tap. Figure 4 plots the cumulative distribution function (*cdf)* of the eigenvalues of channel models 'A', 'B', and 'F' for 4×4 MIMO UCA based system. It is known that the steeper slope the *cdf* curve has the less amplitude of the fluctuation in the signal, i.e., the fades due to the multipath are less deep, and therefore a higher degree of diversity is obtained.

Fig. 3. $R_s(21,11)$ for different taps of model 'F' versus UCA radius in the receiver.

Figure 4 illustrates the impact of each sub-channel, identified in, upon the total capacity available for different channel models. As can be seen, the largest eigenvalue characteristic (λ_1) is nearly the same for most of the channel models. However, the difference increases between models 'A', 'B' and 'F' is more distinguished for 2nd, 3rd, and 4th eigenvalues, respectively. According to (10), the higher summation of eigenvalues the higher capacity, thus as shown in the Fig. model 'F' has the highest summation of eignvalues that leads to the highest capacity. This result was expected due to the high number of clusters and multi-paths components that are included in model 'F' compared to other models.

The capacity dependence on the azimuth rotating of the receiver configuration (orientation of AP) with respect to different channel models is studied. The rotation is measured by the orientation angle (θ_r) shown in Fig.1 with respect to a reference angle ϕ_1 that is used as a reference

for the prescribed AoAs defined by the *TGn* models. Two cases are considered: case (1): 4×4 UCA×UCA based system radii R_t, $R_r=0.75\lambda$ and case (2): 4×4 ULA×ULA Based system with inter-element distance $d_t=0.5\lambda$. To have fair comparison these dimensions are assumed to have identical largest array dimension equal to 1.5λ for both cases. The results are demonstrated in Fig. 5. The presented results reveal that the ergodic capacity in general is more affected by the orientation angle in the ULA unlike in the UCA. This effect gives a privilege to the use of the UCA receiver. Also, as can be observed that the mean capacity for different models (A, B, C, and F) and configurations (ULA and UCA) is compared to the mean 4x4 (i.i.d) MIMO capacity. The independent and identically distributed (i.i.d) case is considered for uncorrelated channel case where channel matrix elements is modeled as i.i.d. zero-mean unit-variance complex Gaussian random variables. Capacity for this case is found to be =10.823 b/s/Hz. As expected for Model 'A' ULA configuration, since the Model A has only one tap one cluster at AoA=45°, then by rotating the ULA by 45° the signal will impinge the array from the endfire direction. In this case the correlation will be highest and the capacity will be minimum. In contrary, if the ULA is rotated by 135° we get the maximum capacity because in this case signal arrives at the broadside of the array. Also it can be observed that the capacity of model F is almost constant and it has the highest values for both configurations. Model B for ULA has the lowest throughput values. UCA case the mean capacity is approximately between a minimum of 77% of the mean 4x4 i.i.d. MIMO capacity (for model C at angle 135°) and a maximum of 96% of the mean 4x4 i.i.d. MIMO capacity (for model F at angle 67.5°). However, the ULA case, the mean capacity is approximately between a minimum of 62% of the mean 4x4 i.i.d. MIMO capacity (for model B at angle 157.5°) and a maximum of 95% of the mean 4x4 i.i.d. MIMO capacity (for model F at angle 90). Here, it can be concluded that, the variations range of ergodic capacity for UCA-MIMO configuration over various orientations and different channel conditions is higher than that for ULA-MIMO configuration under the same orientations and channel conditions.
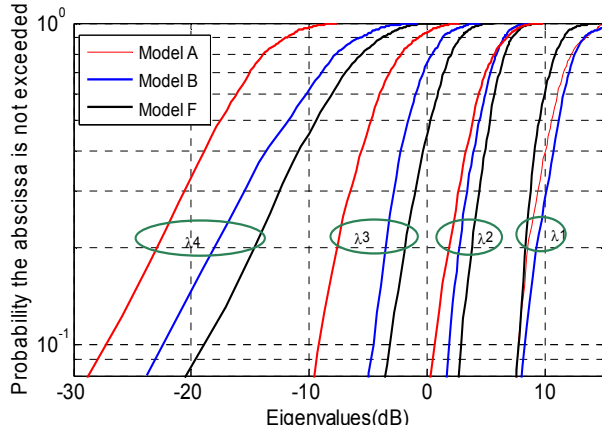
Fig. 4. Channel singular values CDFs of models A, B, and F for 4×4 MIMO UCA based system.
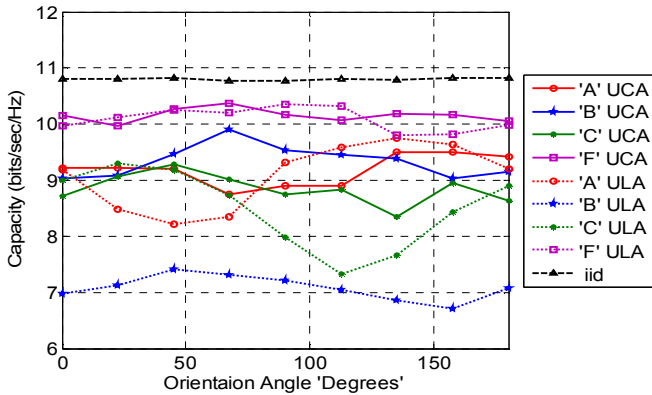

Fig. 5. Ergodic capacity versus azimuth orientation angle at receiver side cases 1 and 2, NLOS conditions.

Figure 6 presents the ergodic capacity versus UCA radius for channel models 'A', 'B', and 'F. For each model, the capacity is investigated at M_r = 2, 4, and 8. The capacity of model 'F' has the highest value for all cases because of the 18 taps and 6 clusters arriving to the UCA array from different AoAs. One tap, one cluster model 'A' found to be the lower bound for all cases. As can be seen, for 'A', 'B', and 'F' models, the values of mean capacity are, respectively, 5.4, 5.75, and 5.9 (for M_r = 2) and 12.14, 12.95, and 15.13 (for M_r= 8). These results show that as M_r increases, the capacity values are more affected by the model selection. This indicates that, the environment profiles should be carefully modeled and selected whenever capacity investigations are performed in particular for higher order MIMO.
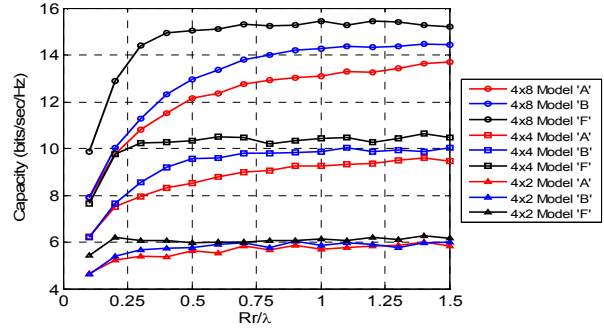

Fig. 6. Ergodic capacity versus radius of channel models 'A', 'B', and 'F' for M_t=4, M_r=2, 4, 8 and SNR=10 dB.

Next, LOS conditions for UCA based MIMO systems are examined by assuming that the LOS component will be included if the separation between the transmitter mobile unit and the receiver AP are within breakpoint distance. The LOS is configured by adding a standard K-factor reported in [7] to the first tap while all the other taps K-factor remain at -∞ dB as in IEEE802.11n model. The LOS component of the first tap is added on top of the NLOS component so that the total energy of the first tap for the LOS channels becomes higher than the value defined in the power delay profiles (PDP). Figure 7 shows the capacity CDFs for a 4x4 UCA based MIMO under A, B, and F channel scenarios for both LOS and NLOS cases. As noticed from the figure, the LOS component degrades the capacity of the system working in all channel scenarios. It is found that in NLOS conditions, capacity improves by 20% compared to the case where the LOS component included. The improvement is less pronounced for model F than other models due to its many multipath taps thus the effect of the 1st LOS tap will be less significant.

Capacity results for the UCA based MIMO systems that apply the water-filling (WF) scheme under different channel conditions are shown in Figs. 8 and 9. In the WF scheme, the power allocated to each sub-channel is optimized to maximize the system capacity. Figure 8 shows ergodic capacities versus SNR for channel models 'A', 'B', 'C', and 'F' for 4x4 UCA based MIMO system. Identical with the results of i.i.d uncorrelated channel model [1], the capacity delivered by the WF power allocation scheme is superior to the one achieved with uniform power specifically for low SNRs. As shown, the capacity

increase by applying the WF scheme is found to be in 'A' and 'C' models more than that for 'B' and 'F' models. Figure 9 shows the capacity versus the number of elements of the UCA (M_r) at the receiver for $4 \times M_r$ MIMO system both uniform and WF schemes values when varying the channel models. As seen, when the number of receiver elements is greater than 3 the capacity becomes more dependent on the environment profiles. It is noticed that in general as the number of received antennas increases the capacity increases for the uniform scheme. However, for models 'A' and 'C' the WF algorithm gets its best performance at $M_r =$ 4 and in general when the numbers of antennas at the transmitter and at the receiver are equal, i.e. the channel matrix is full rank.
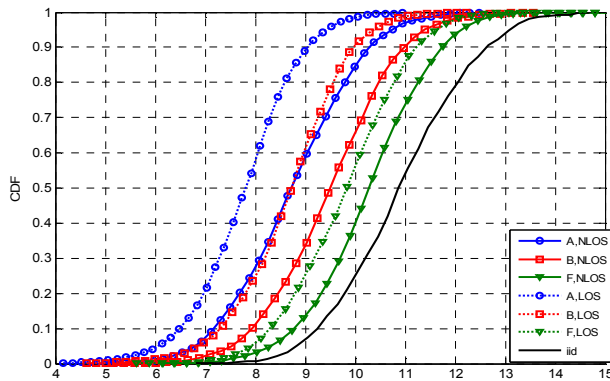

Fig. 9. Ergodic capacities of channels 'A', 'B', 'C', and 'F' versus the number of received antennas, for $4 \times M_r$ UCA based system with uniform and water-filling power schemes.

Fig. 7. Cumulative distribution functions (CDFs) of capacity for models 4x4 UCA based MIMO in 'A', 'B', and 'F' channel models with and LOS and NLOS conditions.
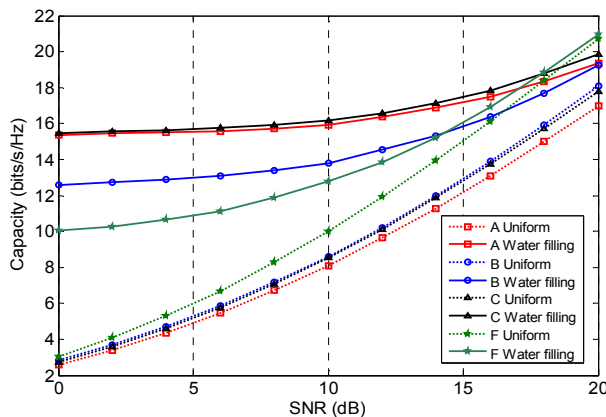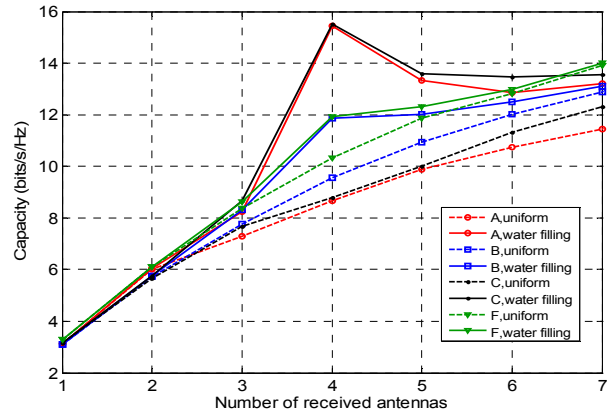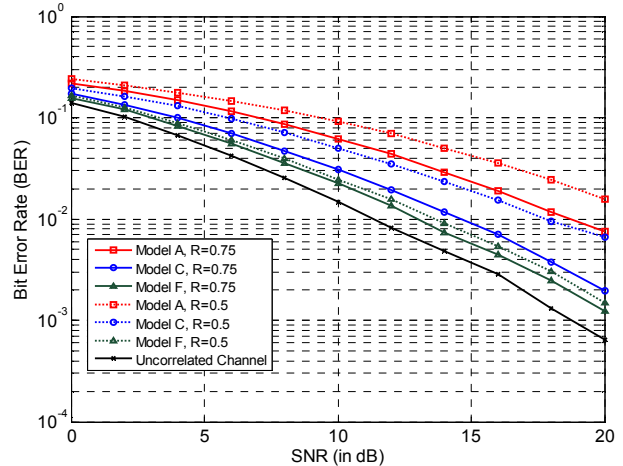

Fig. 10. BER performance of VBLAST MIMO system for three models 'A', 'C' and 'F' compared to uncorrelated channel model with BPSK and various 4x4 UCA radii.

Fig. 8. Ergodic capacity versus SNR of channel models 'A', 'B', 'C', and 'F' for 4x4 UCA-MIMO.

Finally, the diversity gain measured by bit error rate (BER) performance is examined for WLAN 802.11n system utilizing minimum mean squares estimation- VBLAST (MMSE-VBLAST) system [15] with UCA configurations. Two radii R=0.5λ and 0.75λ are considered at the AP receiver. Figure 10 illustrates a comparison of BER performance curves under different *TGn* models. Corresponding BER of an i.i.d. channel (uncorrelated fading channel) is also included for comparison. As can be seen that the link has its best performance for Model 'F' conditions, in this case it is the nearest performance curve to the

uncorrelated fading channel 'i.i.d' curve. Model 'F' performance curve is followed by model 'B' then model 'A' with the lowest performance. Also, as expected that the link performance improves as the radius of the UCA at the AP end increases from 0.5λ to 0.75λ. In general, the results show that the BER performance of uniform circular diversity array depends on the main AoA.

V. CONCLUSION

In this paper, a modification to IEEE 802.11*n* channel model has been proposed to consider the application of using the UCA configurations in MIMO WLAN systems. Realistic spatio-temporal channel model has been developed and includes spatial fading correlation for six different environment profiles. Each profile is distinguished by its predefined parameters such as number of clusters, number of taps within each cluster, power delay profile of the taps, and angle of incidence of each tap. The impact of the selection of realistic channel profile on the eignvalue of each sub-channel and the total system capacity values has been studied. The capacity dependence on the used ULA or UCA geometries and their orientations at both ends of the MIMO system has been studied and compared. It has been found that, the variation range of ergodic capacity for UCA-MIMO configuration over various orientations and different channel conditions is higher than that for ULA-MIMO configuration under the same orientations and channel conditions. The influence of the LOS component on the link performance was presented for UCA based systems and it is shown that LOS component existence is not preferable for MIMO systems. The improvement is less pronounced for large space model F environments. Both uniform and none uniform WF power allocation schemes have been simulated for UCA based systems and it can be said that the WF relocation power scheme is best applied for MIMO UCA based systems working in residential models A and C environments. Moreover, VBLAST system BER performance has been investigated under different channel scenarios and the results show that its best conditions for having the best UCA-MIMO system performance are model F conditions. Finally, the realistic channel model that is introduced in this paper could be effectively utilized to provide an accurate capacity and system performance analysis for the next generation WLANs.

REFERENCES

[1] M. Jankiraman, "Space-Time Codes and MIMO Systems", Artech House Publishers, Boston, London.

[2] A. Saleh and R. Valenzuela, "A Statistical Model for Indoor Multipath Propagation," *IEEE J. Sel. Areas Comm.*, vol. 5, no. 2, pp.128–137, Feb. 1987.

[3] Q. Spencer, M. Rice, B. Jeffs, and M. Jensen, "A Statistical Model for Angle of Arrival in Indoor Multipath Propagation," *Proc. IEEE Veh. Technol. Conf.*, vol. 3, pp. 1415–1419, May 1997.

[4] L. Schumacher, K. I. Pedersen, and P. E. Mogensen, "From Antenna Spacings to Theoretical Capacities - Guidelines for simulating MIMO systems," *Proc. PIMRC Conf.*, vol. 2, pp. 587-592, Sep. 2002.

[5] J. P. Kermoal, L. Schmacher, P. Mogensen, and K. I. Pederson, "Experimental Investigation of Correlation Properties of MIMO Radio Channels for Indoor Picocell Scenarios", in proc. IEEE Vehicular Technology conference, Boston, USA, vol. 1, pp. 14-21, Sept. 2000.

[6] 3GPP, "Spatial Channel Model for MIMO Simulations," TR25.996 V6.1.0, Sep. 2003.

[7] IEEE P802.11 Wireless LANs, "TGn Channel Models," *IEEE* 802.11-03/940r4, 2004-05-10.

[8] J. Tsai, R. M. Buehrer, and B. D. Woerner, "Spatial Fading Correlation Function of Circular Antenna Arrays with Laplacian Energy Distribution," *IEEE Comms. Letters*, vol. 6, no. 5, pp.178-180, May 2002.

[9] L. Xin and Z.-P. Nie, "Spatial Fading Correlation of Circular Antenna Arrays with Laplacian PAS in MIMO Channels," *International Symposium of IEEE Antennas and Propagation Society*, vol. 4, pp. 3697–3700, 2004.

[10] A. Forenza, D. J. Love, and R. W. Heath, "Simplified Spatial Correlation Models for Clustered MIMO Channels with Different Array Configurations," *IEEE Transactions*

on Vehicular Technology, vol. 56, no. 4, pp. 1924-1934, July 2007.

[11] Dantona, V., Schwarz, R.T., Knopp, A., Lankl, B., "Uniform Circular Arrays: The Key to Optimum Channel Capacity in Mobile MIMO Satellite Links," *5th Advanced satellite multimedia systems conference*, pp. 421-428, 13-15 Sept. 2010.

[12] Suzuki, H., Hayman, D.B., Pathikulangara, J., Collings, I.B., Zhuo Chen, and Kendall, R., "Design Criteria of Uniform Circular Array for Multi-User MIMO in Rural Areas," *IEEE Wireless Communications and Networking Conference*, pp. 1-6, April 18-21 2010.

[13] Bu Hong Wang and Hon Tat Hui, "Investigation on the FFT-Based Antenna Selection for Compact Uniform Circular Arrays in Correlated MIMO Channels," *IEEE Transactions on Signal Processing*, vol. 59, no. 2, pp. 739-746, Feb. 2011.

[14] M. A. Mangoud "Capacity Investigations of MIMO Systems in Correlated Rician Fading Channel Using Statistical Multi-Clustered Modeling," *Applied Computational Electromagnetics Society (ACES) Journal*, vol. 25, no. 2, 2010.

[15] D. Chizhik, et. al., "Effect of Antenna Separation on the Capacity of BLAST in Correlated Channels," *IEEE Comm. Lett.*, vol. 4, pp. 337–339, Nov. 2000.